

Doxorubicin Immobilization on Chitosan-modified Silver Nanoparticles as a Drug Delivery Method for Effective Anticancer Treatment

Manar S. Jabar, Shatha Abdul Wadood AL- Shammaree*

Department of Chemistry, College of Science, University of Baghdad, Baghdad, Iraq.

Correspondence to: Shatha Abdul Wadood AL-Shammaree (E-mail: shath_a@sc.uobaghdad.edu.iq)

(Submitted: 01 February 2022 – Revised version received: 20 February 2022 – Accepted: 03 March 2022 – Published online: 26 April 2022)

Abstract

Objectives: The goal of this research is to load Doxorubicin (DOX) on silver nanoparticles coupled with folic acid and test their anticancer properties against breast cancer.

Methods: Chitosan-Capped silver nanoparticles (CS-AgNPs) were manufactured and loaded with folic acid as well as an anticancer drug, Doxorubicin, to form CS-AgNPs-DOX-FA conjugate. AFM, FTIR, and SEM techniques were used to characterize the samples. The produced multifunctional nano-formulation served as an intrinsic drug delivery system, allowing for effective loading and targeting of chemotherapeutics on the Breast cancer (AMJ 13) cell line. Flowcytometry was used to assess therapy efficacy by measuring apoptotic induction.

Results: DOX and CS-AgNPs-DOX-FA were found to inhibit cell proliferation in the AMJ13 cell line, according to the findings. The anti-proliferative impact of these chemicals was attributed to cell death and activation of apoptosis, as evidenced by dual staining with acridine orange and Ethidium bromide. The presence of high fluorescent signals specific for cellular uptakes of CS-AgNPs-DOX-FA into the cell line's cytoplasm was confirmed.

Conclusion: According to the findings of this study, CS-AgNPs-DOX-FA has a lot of promise to be used as an anticancer delivery system. The findings imply that this conjugate should be researched further for potential use as anticancer drug.

Keywords: Chitosan, Doxorubicin, Folic Acid, cellular uptake

Introduction

Cancer can be defined as a disease in which a group of malignant tumors grows out of control, defying the convention rules of cell division.¹ Cells are traditionally governed by signals that indicate whether the cell should proliferate; develop further into a cell, or death.² After heart disease, cancer is the second leading cause of mortality.³ Doxorubicin (DOX) is a medication that is often used to treat cancers such as ovarian carcinoma, leukemia, colon cancer, breast cancer, lung cancer, and prostate cancer, as well as other lymphomas. Doxorubicin has a number of negative side effects in humans, such as nephrotoxicity and cardiac toxicity.⁴ As a result, efforts have been made to create new DOX delivery techniques in order to lessen these side effects, which could alter DOX's biological distribution, promote its deposition at cancer locations, and improve its therapeutic effectiveness. Drug delivery is a science that uses approaches that are based on biology, chemistry, engineering, and medical principles.⁵

Nanoparticles could represent a breakthrough in the treatment of a variety of disorders.⁶ Due to their diverse uses like anti-bacterial, anti-cancer, anti-inflammatory, biocatalysis, and biosensor, silver nanoparticles are one of the most commonly utilized nanomaterials.⁷ Nano-machines and nanoparticles can multiply themselves due to their design, making them an affordable and accessible therapy option for a larger population.⁸ It can also aid in the development of smart drug-loaded nanoparticles, which can result in more accurate drug delivery, increased efficacy, and lower toxicity.⁹

While exploiting its effective anti-cancer properties; an ideal targeted DOX delivery mechanism would reduce required doses as well as the prevalence and degree of adverse effects associated with the medicine.¹⁰

Chitosan is the second most abundant natural polysaccharide formed from chitin,¹¹ its features include non-toxicity, biocompatibility, antibacterial activity, and biodegradability,¹² and there are few of the pharmacological and biological applications where it performs¹³ such as tissue engineering,¹⁴ drug delivery,¹⁵ and wound-healing dressing.¹⁶ After cellulose, chitosan comes in second where combining chitosan with AgNPs to generate nano-hybrids of silver and chitosan is particularly promising for antibacterial and anti-cancer applications.¹⁷

Folic acid (vitamin B9) is an important component of cell development and metabolism, and because of its high affinity for the folate receptor proteins; folate is used as a cancer-targeting agent, because folate receptor is overexpressed in certain malignant cells such as breast, ovarian, lung, kidney, brain, and colon cancers and it's considered as a tumor biomarker.¹⁸ When folate is conjugated with drug delivery methods; it improves the drug uptake via endocytosis in cells.¹⁹ Researchers have used this technique to create the surface of nanoparticles that contains folic acid.²⁰

The goal of this research is to develop and test the ability of the CS-AgNPs-DOX-FA combination to deliver anticancer drugs more effectively on breast cancer cell line.

Materials and Methods

Chemicals and Reagents

Chitosan (CS) (CDH India), Acetic acid (Solvochem UK), Silver nitrate (AgNO₃) (Avonchem UK), Sodium hydroxide (NaOH) (Panreac Spain), Acridine Orange–Ethidium bromide (AO/EtBr; Sigma–Aldrich, USA), Dual Staining (Sigma USA), Dimethyl Sulfoxide (Santacruz Biotechnology, USA), Fluorescein Isothiocyanate Isomer I (FITC) (Sigma USA), RPMI-1640 Media (Capricorn Germany), Trypsin, breast

cancer cell line (AMJ 13), 3-(4,5-Dimethyl-2-thiazolyl)-2,5-diphenyl-2H-tetrazolium bromide (MTT) (Bio-World USA).

Preparation of Silver Nanoparticles with Chitosan (CS-AgNPs)

In common synthesis of silver nanoparticle, 1 g of chitosan was dissolved in 5% acetic acid with stirring for 30 min. This was then filtered to achieve clear solution. About 15 mL of freshly 0.1 M AgNO₃ was added followed by the addition of one hundred µL of 1 M NaOH and stirring for 10 h at 90°C. The color was turned from colorless to light yellow and subsequently to yellowish brown which confirm the formation of CS-AgNPs.²¹

Preparation of CS-AgNPs-DOX-FA (Conjugate)

One mg of DOX was added to 10 ml of CS-AgNPs and mixed for 24 hours at 37°C for DOX loading. Using a calibration curve and an excitation wavelength of 480 nm, the amount of DOX in the supernatant was quantified spectrofluorometrically and a 575 nm emission wavelength for every 1 ml of hybrid CS-AgNPs surface formation, then 50 micrograms of DOX were injected (CS-DOX -AgNPs).

A 10 mg dose of folic acid (FA) was added to the solution and stirred at room temperature for another day in the dark.²²

Characterization of Silver Nanoparticles and CS-AgNPs-DOX-FA Conjugate

Fourier Transform Infrared (FT-IR) Spectroscopy

To identify the functional groups in the samples, FTIR equipment (Shimadzu Corporation, Japan) was used to scan them over a wavelength range of 400–4000 nm.

Atomic-force Microscopy (AFM)

The AFM was used for the determination of surface morphology, thickness, roughness, and topography of the materials. The measure of the thickness of the film is carried out by the careful scratching of the film in representative area. The physical AFM operation is involved with a cantilever that as a sharp tip with high sensitivity to the small forces, making contact with sample surface.²³

Field Emission Scanning Electron Microscopic (FESEM)

The morphology and nanoparticle grain size of the examined materials were seen using a scanning electron microscope (SEM). By lowering the amount of solution on the cover slide grid, thin films of silver nanoparticles and the CS-AgNPs-DOX-FA conjugate were formed, which were then allowed to dry at room temperature before being seen under SEM.

The *in vitro* Study

Cytotoxicity Assay

To determine the cytotoxic effect of DOX and CS-AgNPs-DOX-FA conjugate, the 3-(4,5-Dimethyl-2-thiazolyl)-2,5-diphenyl-2H-tetrazolium bromide (MTT) assay was done using 96-well plates.^{24,25} A 1 × 10⁴ cells/well was seeded from the Breast cancer cell line. After 24 hours or the formation of a confluent monolayer, cells were treated with DOX and CS-AgNPs-DOX-FA conjugate by adding (1.5, 3.1, 6.25, 12.5, 25 µg/ml) to the wells. By removing the medium, 28 µL of

2 mg/mL MTT solution was added, followed by incubation of the cells for 2.5 hours at 37°C, cell viability was determined after 24, 48, and 72 hours of last addition. After removing the MTT solution, the crystals in the wells were solubilized by adding 130 µL of DMSO followed by incubating with shaking at 37°C for 15 minutes.²⁶ The absorbency was measured at 492 nm using a microplate reader, and the test was done in triplicate. The following equation was used to compute the rate of cell growth inhibition (the percentage of cytotoxicity):

$$\text{Inhibition rate} = A - B/A \times 100$$

Where A is the optical density of control, and B is the optical density of the samples.

The cells were then treated for 24 hours to DOX and CS-AgNPs-DOX-FA conjugate. The plates were stained with crystal violet stain and incubated at 37°C for 10–15 minutes after the exposure duration. The stain was carefully wiped away with tap water until all of the dye was gone. The cells were viewed under a 100 magnification inverted microscope, and photos were recorded with a digital camera mounted to the microscope.

Apoptosis Assay (AO/EtBr)

The Acridine Orange–Ethidium bromide (AO/EtBr; Sigma–Aldrich, USA) staining method was used to examine the DOX and CS-AgNPs-DOX-FA conjugate induced mortality of the AMJ13 cell line. Briefly, 24 hours after seeding cells in 12-well plates, they were treated with DOX and CS-AgNPs-DOX-FA conjugate at IC₅₀ (14.67 g/ml and 11.03 g/ml, respectively) and incubated for an additional 20 hours. Phosphate-buffered saline was used to wash the cells twice. At an equal number of cells, dual fluorescent dyes (10 µL of AO/EtBr) were applied to the wells. Finally, fluorescent microscopy was used to examine the cells.²⁷

Fluorescent Labeling using FITC

The following procedure was used to make the CS-AgNPs-DOX-FA conjugate tagged with a fluorescent dye; Fluorescein Isothiocyanate Isomer I (FITC) (1 mg mL⁻¹) was mixed with CS-AgNPs-DOX-FA conjugate and incubated at room temperature for 10 hours. The cells were treated at 37°C for 12 hours with the FITC-labeled CS-AgNPs-DOX-FA combination. The nuclei were stained with DAPI labeling. A fluorescent microscope was used to take images at a magnification of 40.²⁸

Statistical Analysis

The analysis of data was statistically evaluated using Graph Pad Prism 6, and an unpaired *t*-test was used. The mean and standard deviation of three measurements were used.

Results and Discussion

Characterization of CS-AgNPs-DOX-FA

Fourier Transforms Infrared Spectroscopy Analysis

Compounds' FTIR spectra were collected in the wavelength range 4000–400 cm⁻¹. There is an overlapping of O-H stretching and N-H stretching bands in pure chitosan, which contributes

to the development of a peak around 3430 cm^{-1} , as reported by Hassan M. Ibrahim et al. 2018.²⁹ In the CS-AgNPs spectra, this characteristic peak shifted to 3428 cm^{-1} . The C-H stretching and C-H bending peaks of pure chitosan occurred at 2917 cm^{-1} , and 1426 cm^{-1} , respectively, in the CS-AgNPs spectra. These two peaks are also displaced to 2925 cm^{-1} , and 1418 cm^{-1} , respectively, in the CS-AgNPs spectrum. N-H bending produced a distinctive peak at 1637 cm^{-1} , which shifted to 1625 cm^{-1} in the CS-AgNPs spectra.³⁰ The overlapping of the

alcoholic C-O stretching band and the ether linkage, as well as the C-O-C stretching band, resulted in a peak at 1079 cm^{-1} (Fig. 1b) while, in the CS-AgNPs spectra, this peak emerges at 1080 cm^{-1} (Fig. 1b). These findings are in line with those of prior investigations of studies by other researchers.^{31,32} FTIR spectra for both CS-AgNPs-DOX and DOX were used to validate DOX loading on CS-AgNPs (Fig. 1c). DOX characteristic peaks may be seen in Fig. 2b at 3382 cm^{-1} , and 1618 cm^{-1} .^{33,34} The FTIR spectra of CS-AgNPs-DOX indicated a frequency

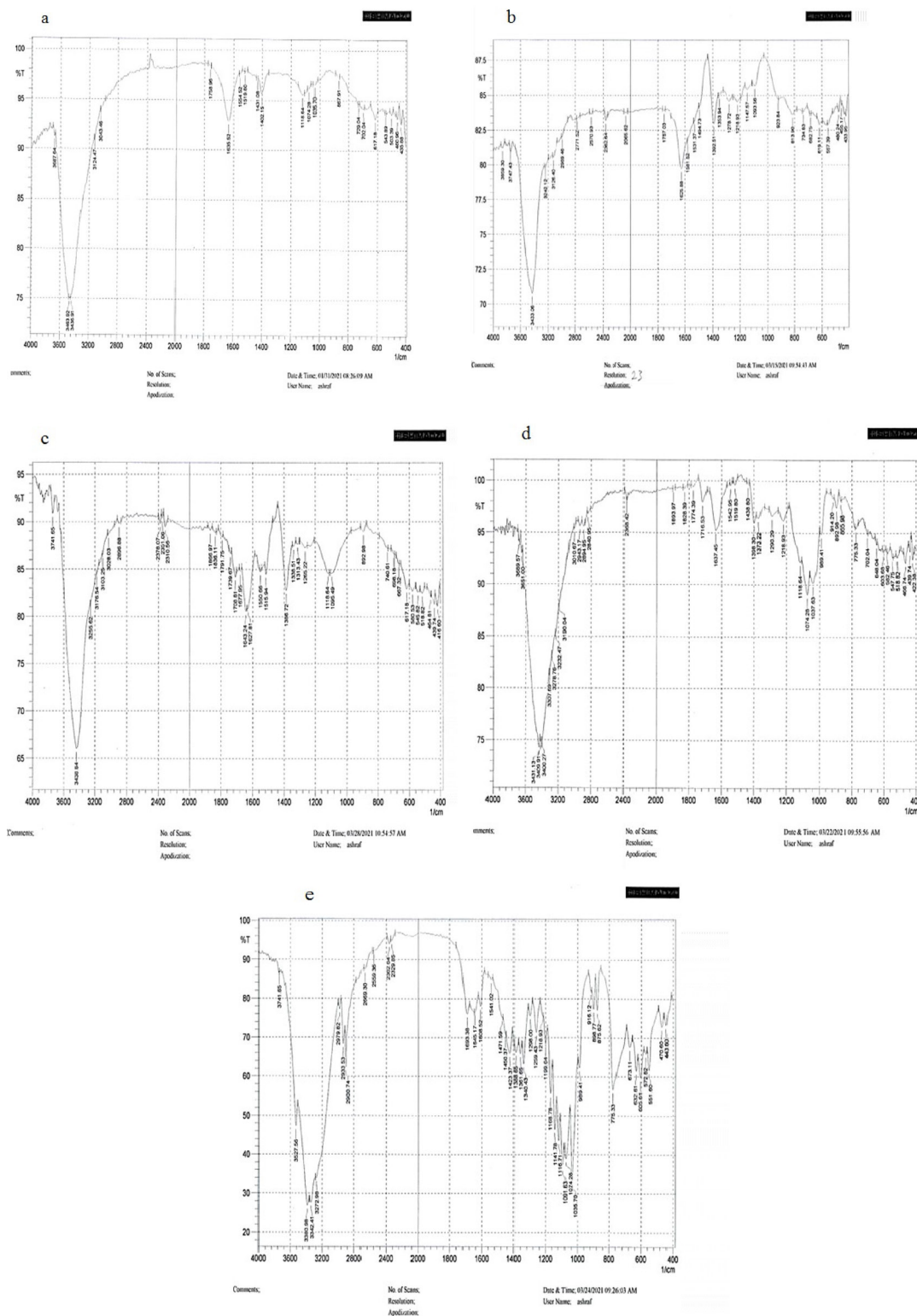


Fig. 1 (a) FTIR of Chitosan. (b) FTIR of DOX-AgNPs. (c) FTIR of CS-AgNPs-DOX-FA. (d) FTIR of DOX. (e) FTIR of FA.

shift in DOX characteristic peaks to 3428 cm^{-1} , 1639 cm^{-1} , as well as a considerable decrease in intensity, after DOX loading on CS-AgNPs (Fig. 1d). The interaction of DOX's negative carboxylate group with the positive amino group of chitosan which coats the surface of silver nanoparticles is the cause this change. These findings support the developed nano-stability hybrid.³⁵

The FTIR spectra of FA, CS, and FA-CS conjugates are illustrated in the diagram (Fig. 1c). The hydroxyl ($-\text{OH}$) stretching and $\text{N}-\text{H}$ stretching vibrations emerged as peaks in FA (Fig. 1e) between 3600 and 3000 cm^{-1} . The $\text{C}=\text{O}$ stretching vibration of the $-\text{COO}$ group appeared at 1692 cm^{-1} , while the $\text{C}=\text{O}$ bond stretching vibration of the $-\text{CO}-\text{NH}$ group appeared at 1640 cm^{-1} . The bending mode of $\text{N}-\text{H}$ vibration showed at 1605 cm^{-1} , while the $-\text{OH}$ deformation band of the phenyl structure appeared at 1412 cm^{-1} . At 1483 cm^{-1} , the phenyl ring's distinctive absorption peak appeared.³⁶ The stretching vibrations of $\text{N}-\text{H}$ (3456 cm^{-1}) and $\text{C}-\text{H}$ stretch vibrations (2884 and 2846 cm^{-1}) functional groups were discovered in the FTIR spectra of CS (Fig. 1a). Amide I, II, and III each had peaks at 1664 , 1592 , and 1324 cm^{-1} , respectively. Peaks at 1420 cm^{-1} , and 1383 cm^{-1} were indicative of $-\text{CH}_3$ symmetrical deformation, while peaks at 1152 cm^{-1} , and 1087 cm^{-1} were indicative of $\text{C}-\text{O}$ stretching vibrations from $(\text{C}-\text{O}-\text{C})$.³⁷ The characteristic absorption bands of both FA and CS were visible in the FTIR spectra of the FA-CS conjugate (Fig. 1c). The presence of chemical interactions between FA and CS was established when the peak due to the deformation vibration $\text{N}-\text{H}$ amide-II of the amine group (1597 cm^{-1}) changed to a higher frequency at 1605 cm^{-1} . Furthermore, the amide-III (1324 cm^{-1}) and $\text{C}-\text{O}$ stretching

vibrations (1087 cm^{-1}) peaks of CS were moved to 1312 cm^{-1} , and 1078 cm^{-1} , respectively, implying that FA and CS may interact strongly.

Atomic-force Microscopy Analysis

The 3D AFM image distribution of silver nanoparticles and CS-AgNPs-DOX-FA is shown in Fig. 2. The silver nanoparticles appeared to be spherical, with a grain size of up to 7 nm , according to the photograph.

Scanning Electron Microscope

The size and shape of the compounds were seen using the SEM method. Figure 3 shows the findings of SEM characterization of the produced silver nanoparticles. The SEM image revealed nanoparticles with a diameter range of $>10\text{ nm}$ that were substantially spherical in shape.

The Anticancer Activity

The MTT Assay

The cytotoxic effect of DOX and CS-AgNPs-DOX-FA conjugate against Breast cancer cell line was studied. The anti-proliferative activity of the DOX and CS-AgNPs-DOX-FA conjugate was tested by *in vitro* study of their ability to inhibit the proliferation of (AMJ13) cell line but not normal cell line (HBL-100) cells. The results of this study showed the cytotoxic activity of DOX and CS-AgNPs-DOX-FA conjugate against the AMJ13 cell line and the results revealed a concentration dependent manner, as shown in Figures 4–7.

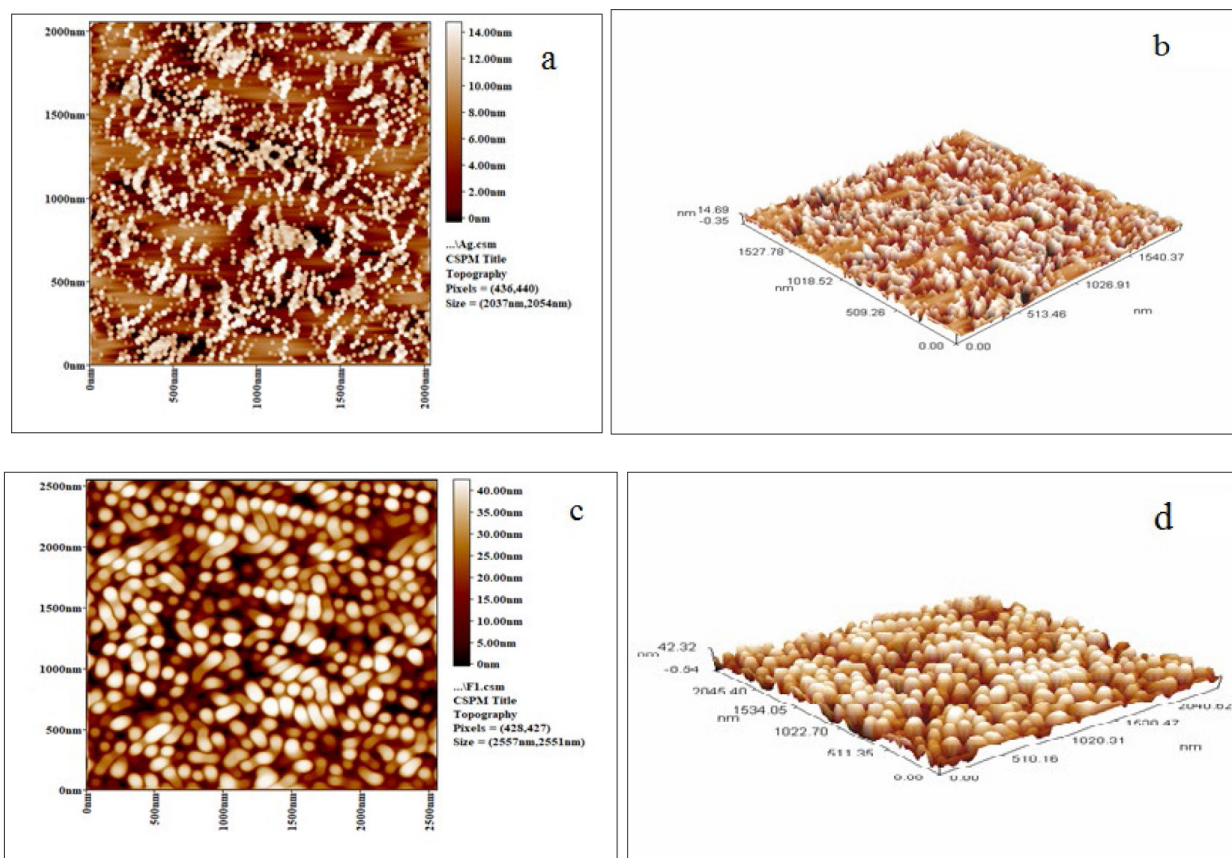


Fig. 2 (a, b) AFM images of synthesized of AgNPs, (c, d) AFM images of synthesized of CS-AgNPs-DOX-FA.

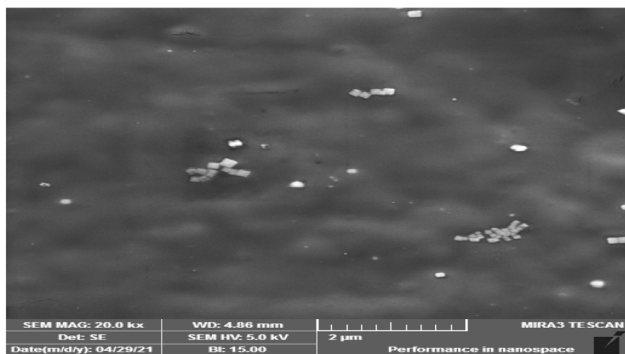


Fig. 3 The SEM image of CS-AgNPs-DOX-FA.

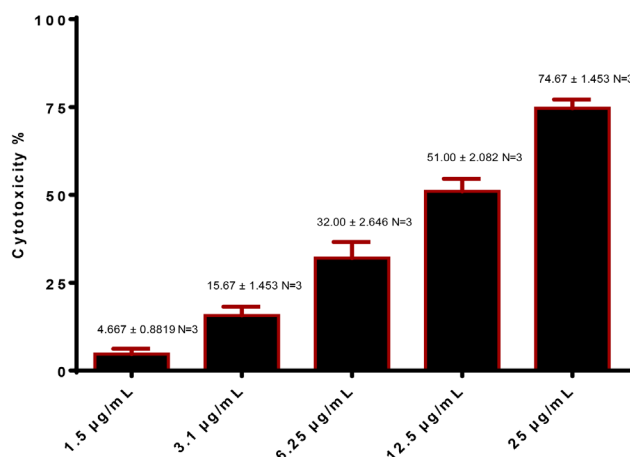


Fig. 4 Cytotoxic effect of DOX in AMJ13 cells. IC₅₀ = 14.67 μg/ml.

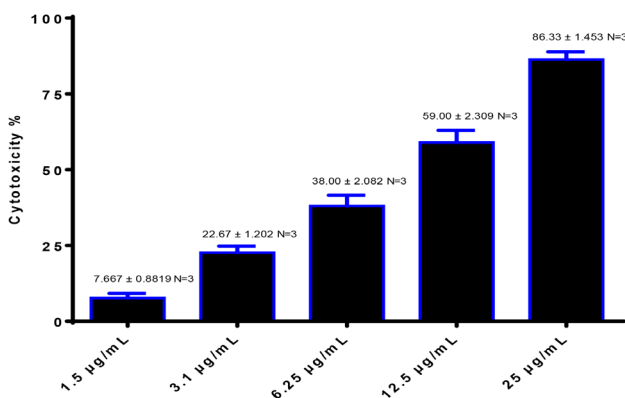


Fig. 5 Cytotoxic effect of CS-AgNPs-DOX-FA conjugate in AMJ13 cells. IC₅₀ = 11.03 μg/ml.

After 48 hours, the proliferation of AMJ 13 was significantly inhibited when compared to untreated control cells, cell growth was dramatically reduced. The AMJ 13 cell line showed minimal cytotoxicity after 48 hours of treatment with DOX at a concentration of 25 g/mL, but the cell line showed moderate cytotoxicity after 48 hours of treatment with the CS-AgNPs-DOX-FA conjugate at the same concentration. This conjugate had no effect on the HBL cell line which leads to suggest that this conjugate could be used as anti-proliferative and cytotoxic agents.

Using an inverted phase contrast microscope, the conjugate's apoptogenic properties were studied by morphological

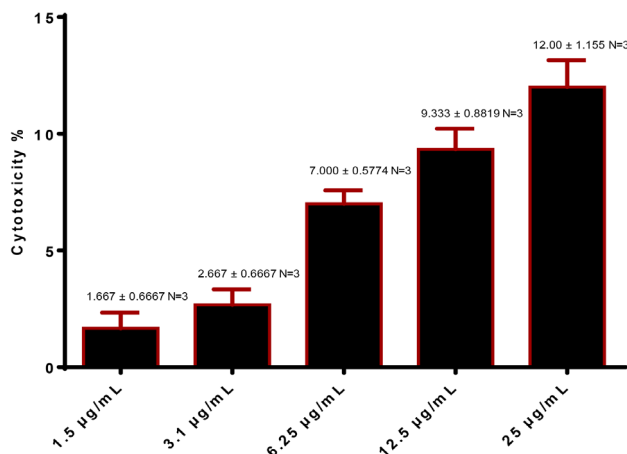


Fig. 6 Cytotoxic effect of DOX in HBL-100 cells.

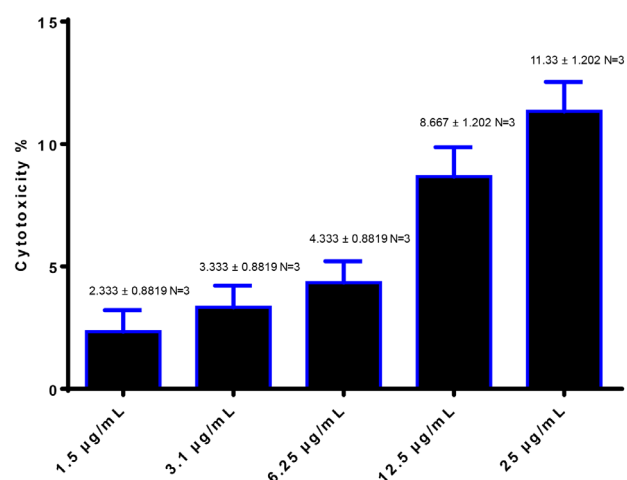


Fig. 7 Cytotoxic effect of CS-AgNPs-DOX-FA conjugate in HBL-100 cells.

alterations in the AMJ13 cell line. The control (untreated) cells retained their original morphology and were generally adhered to the tissue plate, as seen in Fig. 8. After 48 hours of treatment with DOX and CS-AgNPs-DOX-FA conjugate, the cells showed significant anti-proliferative activity and morphological changes. Our findings revealed no morphological alterations in the HBL cell line after treatment with the same conjugate at the same concentration (Fig. 9). Apoptotic signs such as membrane blebbing and lack of contact with neighboring cells were identified, as well as a decrease in the number of cells. This indicates that the nanoparticles may have *in vivo* applications.³⁸

Apoptosis Assay (AO/EtBr)

The changes in the nuclear morphology of AMJ 13 cells after treatment with DOX and CS-AgNPs-DOX-FA conjugate were studied using AO/EtBr dual staining method. The apoptotic cells were evaluated based on DNA damage, as shown in Fig. 10.

Cellular Uptake

A fluorescent microscope was used to visualize the conjugation of FITC to CS-AgNPs-DOX-FA and their cellular absorption, as illustrated in Fig. 11. The presence of significant

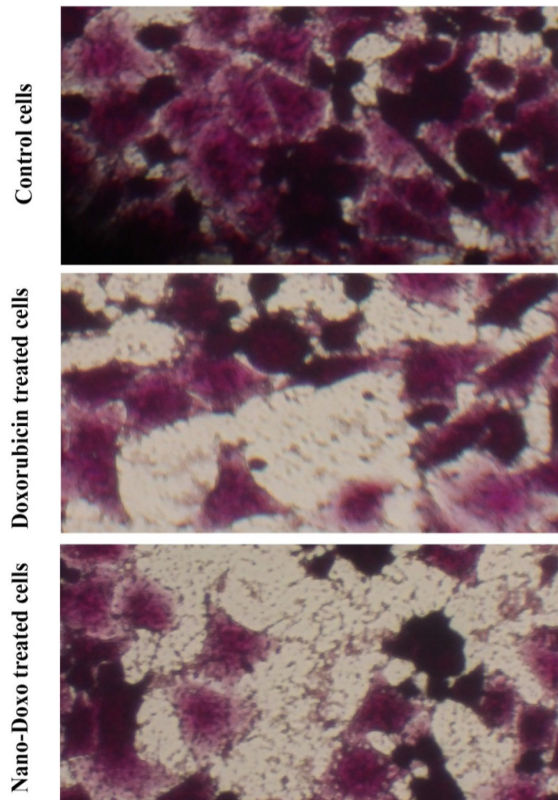


Fig. 8 Morphology changes in AMJ13 cells after treatment with DOX, and CS-AgNPs-DOX-FA. The cells were observed under an inverted microscope at 100× magnification.

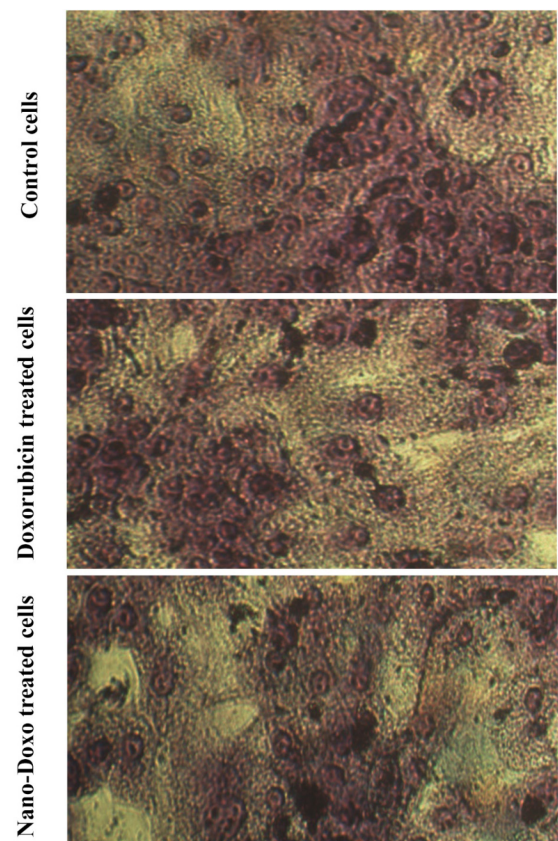


Fig. 9 Morphology changes in HBL-100 cells after treatment with DOX and CS-AgNPs-DOX-FA conjugate. The cells were observed under an inverted microscope at 100× magnification.

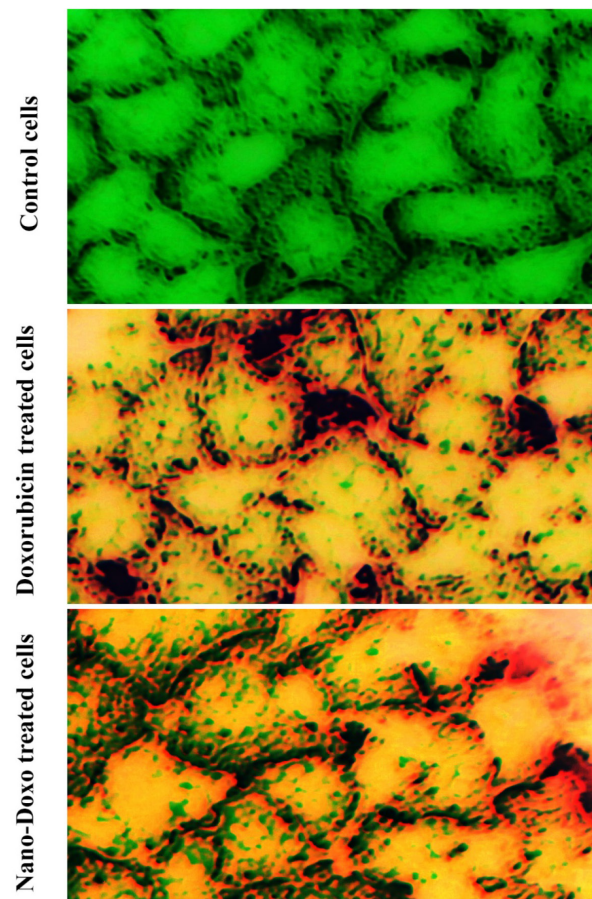


Fig. 10 The induced apoptosis in AMJ13 cell line by DOX and CS-AgNPs-DOX-FA conjugate. Fluorescence microscopic images of AMJ13 cells show the morphological changes after acridine orange-ethidium bromide dual staining. The original magnification is 100X.

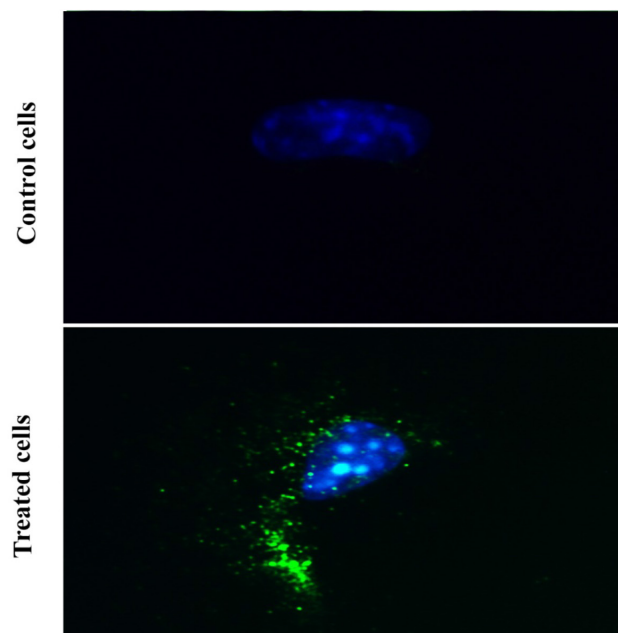


Fig. 11 Cellular uptake of CS-AgNPs-DOX-FA in AMJ13 cells. Control cells mean AMJ13 cells without treatment. Treated cells mean AMJ13 cells treated with CS-AgNPs-DOX-FA. Images were acquired at 100X magnification. The cells were incubated with FITC-labeled CS-AgNPs-DOX-FA conjugate for 24 h at 37°C, 5% CO₂.

fluorescence signals in the treated AMJ13 cells confirmed the selective absorption of this conjugate into the cell's cytoplasm.

Conclusion

This study demonstrates an efficient method for loading doxorubicin onto chitosan modified with AgNPs. The loading method is a simple, cost-effective, large-scale, and energy-efficient way to make well-defined colloidal nanoparticles without using any additives. CS-AgNPs-DOX-FA was also much more cytotoxic on the cancer cell line than DOX alone. According to the findings of this study, CS-AgNPs-DOX-FA

has a lot of promise to be used as an anticancer delivery system. The findings imply that this conjugate should be researched further for potential use as anticancer drug.

Acknowledgment

The authors thank the Iraqi Center for Cancer and Medical Genetic Research for their help in the *in vitro* study spatially Dr. Majid S. Jabir.

Conflicts of Interest

There are no conflicts of interest. ■

References

- National Research N. Council, Reaping the Benefits of Genomic and Proteomic Research: Intellectual Property Rights, Innovation, and Public Health, National Academies Press. 2006 Feb ;15(1):1-188. doi: <https://doi.org/10.17226/11487>
- Cavalier-Smith T. Origin of the cell nucleus, mitosis and sex: roles of intracellular coevolution, Biol. Direct. 2010 Dec; 5(1):1-78. doi:10.1186/1745-6150-5-7
- Jemal A, Siegel R, War E d, Hao Y, Xu J, Murray T, Thun MJ. Cancer statistics, 2008. Cancer J. Clin. 2008 Mar-Apr; 58(2):71-96. doi: 10.3322/CA.2007.0010.
- Elbially N, Mohamed N, Monem AS. Preparation and characterization of SiO₂-Au nanoshells: in vivo study of its photo-heat conversion. Journal of Biomedical Nanotechnology. 2013 Feb; 9(2):158-166. doi: 10.1166/jbn.2013.1481.
- Chen Y, Wan Y, Wang Y, Zhang H, Jiao Z. Anticancer efficacy enhancement and attenuation of side effects of doxorubicin with titanium dioxide nanoparticles. International Journal of Nanomedicine. 2011; 6:2321. doi: 10.2147/IJN.S25460.
- Salehiabar M, Nosrati H, Davaran S, Danafar H, Manjili HK. Facile synthesis and characterization of l-aspartic acid coated iron oxide magnetic nanoparticles (IONPs) for biomedical applications, Drug Res. 2018 May; 68(5):280-285. doi: 10.1055/s-0043-120197.
- Burduşel AC, Gherasim O, Grumezescu AM, Mogoantă L, Ficaï A, Andronescu E. Biomedical applications of silver nanoparticles: an up-to-date overview. Nanomaterials. 2018 Sep; 8(9):681. doi: 10.3390/nano8090681.
- Rostamizadeh K, Manafi M, Nosrati H, H.K. Manjili, H. Danafar, Methotrexate conjugated mPEG-PCL copolymers: a novel approach for dual triggered drug delivery, New J. Chem. 2018 Mar; 42(31):5937-5945. doi:10.1039/C7NJ04864E
- Salehiabar M, Nosrati H, Javani E, Aliakbarzadeh F, H.K. Manjili, S. Davaran, H. Danafar, Production of biological nanoparticles from bovine serum albumin as controlled release carrier for curcumin delivery, Int. J. Biol. Macromol. 2018 Apr; 115:83-89. doi: 10.1016/j.ijbiomac.2018.04.043
- Nosrati H, Sefidi N, Sharafi A, Danafar H, H.K. Manjili, Bovine serum albumin (BSA) coated iron oxide magnetic nanoparticles as biocompatible carriers for curcumin-anticancer drug, Bioorg. Chem. 2018 Feb; 76:501-509. doi: 10.1016/j.bioorg.2017.12.033.
- Elieh-Ali-Komi, D, Hamblin M R. Chitin and chitosan: production and application of versatile biomedical nanomaterials. International Journal of Advanced Research .2016 Mar; 4(3):411-427. doi: 10.1166/jbn.2014.1882.
- Pang Y, Qin A, Lin X, Yang L, Wang Q, Wang Z, Shan Z, Li S, Wang J, Fan S, Hu Q. Biodegradable and biocompatible high elastic chitosan scaffold is cell-friendly both in vitro and in vivo. Oncotarget. 2017 May 30;8(22):35583. doi: 10.18632/oncotarget.14709.
- Naskar S, Sharma S, Kuotsu K. Chitosan-based nanoparticles: an overview of biomedical applications and its preparation. Journal of Drug Delivery Science and Technology. 2019 Feb 1;49:66-81. doi: 10.1080/1061186X.2018.1512112.
- Suh JK F, Matthew HW T. Application of chitosan based polysaccharide biomaterials in cartilage tissue engineering: a review. Biomaterials. 2000 Dec; 21(24):2589-98. doi: 10.1016/s0142-9612(00)00126-5.
- Rajurkar RM, Rathod CP, Thonté SS, Sugave RV, Sugave BK, Phadtare AA, Bhosale PH. Gastroretentive mucoadhesive microsphere as carriers in drug delivery: a review. Indo American Journal of Pharmaceutical Research. 2013Dec; 3(12):2751-2777. <http://www.iajpr.com/index.php/en/>
- Muzzarelli RA. Chitins and chitosans for the repair of wounded skin, nerve, cartilage and bone. Carbohydrate Polymers. 2009 Mar 17;76(2):167-82. <https://doi.org/10.1016/j.carbpol.2008.11.002>.
- Fan Z, Qin Y, Liu S, Xing R, Yu H, Chen X, K. Li, P. Li, Synthesis, characterization, and antifungal evaluation of diethoxyphosphoryl polyaminoethyl chitosan derivatives, Carbohydr. Polym. 2018 Jun 15;190:1-11. doi: 10.1016/j.carbpol.2018.02.056.
- Vollset SE, Clarke R, Lewington S, Ebbing M, Halsey J, Lonn E, Armitage J, Manson JE, Hankey GJ, Spence JD, et al. Effects of folic acid supplementation on overall and site-specific cancer incidence during the randomised trials: meta-analyses of data on 50,000 individuals. 2013 Mar;381(9871):1029-36. doi: 10.1016/S0140-6736(12)62001-7.
- Sabharanjak S, Mayor S. Folate receptor endocytosis and trafficking. Adv Drug Deliv Rev. 2004 Apr;56(8):1099-109. doi: 10.1016/j.addr.2004.01.010.
- Mansoori G. A, Mohazzabi P, McCormack P, Jabbari S, "Nanotechnology in cancer prevention, detection and treatment: bright future lies ahead," World Review of Science, Technology and Sustainable Development. 2007 Jan; 4 (2|3):226-257. doi:10.1504/WRSTSD.2007.013584.
- Sanpui P, Chattopadhyay A, Ghosh SS. Induction of apoptosis in cancer cells at low silver nanoparticle concentrations using chitosan nanocarrier. ACS Appl Mater Interfaces. 2011 Feb;3(2):218-28. doi: 10.1021/am100840c.
- Davaran S, Fazeli H, Ghamkhari A, Rahimi F, Molavi O, Anzabi M, et al. Synthesis and Characterization of Novel P (HEMA-LA-MADQUAT) micelles for co-delivery of Methotrexate and Chrysin in combination cancer chemotherapy. J Biomat Sci Polymer Edition. 2018 Aug; 29(11):1265-1286. doi: 10.1080/09205063.2018.1456026.
- Zapata DA. Design, synthesis, characterization and development of novel organic conducting polymers with technological applications. UPcommons. upc. 2013Jun; 86(3):309-315. URI <http://hdl.handle.net/2117/94880>
- Berridge MV, Herst PM, Tan AS. "Tetrazolium dyes as tools in cell biology: new insights into their cellular reduction". Biotechnology Annual Review. 2005 Sep; 11:127-52. doi: 10.1016/S1387-2656(05)11004-7.
- Stockert JC, Blázquez-Castro A, Cañete M, Horobin RW, Villanueva A. "MTT assay for cell viability: Intracellular localization of the formazan product is in lipid droplets". Acta Histochemica. 2012 Dec; 114(8): 785-796. doi: 10.1016/j.acthis.2012.01.006.
- Salazar C, El-Arabi AM, Scmidt JJ. EC50 and IC50 measurements of TRPM8 in lipid bilayers, Biophysical Journal. 2012 Oct; 102(3): 344-345. doi:10.1371/Journal.pone.0141366
- Sulaiman GM, Jabir MS, Hameed AH. Nanoscale modification of chrysin for improved of therapeutic efficiency and cytotoxicity. Artificial Cells, Nanomedicine, and Biotechnology. 2018 Mar; 46(1): 708-72. doi: 10.1021/bc500452y
- McGarraugh HH. Supramolecular Probes for Imaging, Therapy, and Diagnostics. A Dissertation, University of Notre Dame; 2021.
- Ibrahim HM, Farid OA, Samir A, Mosaad RM. Preparation of chitosan antioxidant nanoparticles as drug delivery system for enhancing of anti-cancer drug. InKey Engineering Materials 2018 (Vol. 759, pp. 92-97). Trans Tech Publications Ltd. <https://doi.org/10.4028/www.scientific.net/KEM.759.92>
- Han D, Yan L, Chen W, Li W. Preparation of chitosan/graphene oxide composite film with enhanced mechanical strength in the wet state.

- Carbohydrate Polymers. 2011 Jan 10;83(2):653-8. <https://doi.org/10.1016/j.carbpol.2010.08.038>.
31. Hajji S, Khedir S B, Hamza-Mnif I, Hamdi M, Jedidi I, Kallel R, Boufi S, Nasri M. Biomedical potential of chitosan-silver nanoparticles with special reference to antioxidant, antibacterial, hemolytic and in vivo cutaneous wound healing effects. *Biochimica et Biophysica Acta (BBA) - General Subjects*. 2019 Jan; 1863(1):241-254. doi: 10.1016/j.bbagen.2018.10.010.
 32. Laghrib F, Ajermoun N, Bakasse M, Lahrich S, El Mhammedi M A. Synthesis of silver nanoparticles assisted by chitosan and its application to catalyze the reduction of 4-nitroaniline. *International Journal of Biological Macromolecules*, 2019 May;135:752-759. doi: 10.1016/j.ijbiomac.2019.05.209
 33. Victor S P, Paul W, Jayabalan M, Sharma CP. Supramolecular hydroxyapatite complexes as theranostic near infrared luminescent drug carriers. *CrystEngComm*, 2014 Aug;16(38):9033-9042. doi:10.1039/C4CE01137F
 34. Nguyen HN, Hoang TM, Mai TT, Nguyen TQ, Do HD, Pham TH, Nguyen TL, Ha PT. Enhanced cellular uptake and cytotoxicity of folate decorated doxorubicin loaded PLA-TPGS nanoparticles. *Advances in Natural Sciences: Nanoscience and Nanotechnology*. 2015 Feb 2;6(2):025005. doi: 10.1088/2043-6262/6/2/025005.
 35. Wazed Ali S, Rajendran S, Joshi M. Synthesis and characterization of chitosan and silver loaded chitosan nanoparticles for bioactive polyester. *Carbohydrate Polymers*. 2001 Jan;83(2):438-446. doi:10.1016/j.carbpol.2010.08.004.
 36. Seifirad S, Karami H, Shahsavari S, Mirabasi F, Dorkoosh F. Design and characterization of mesalamine loaded nanoparticles for controlled delivery system. *Nanomedicine Research Journal*. 2016 Oct 1;1(2):97-106. doi: 10.7508/nmrj.2016.02.006.
 37. Zare, M., Samani, S. M., & Sobhani, Z. Enhanced intestinal permeation of doxorubicin using chitosan nanoparticles. *Advanced Pharmaceutical Bulletin*. 2018 Aug; 8(3):411-417. doi: 10.15171/apb.2018.048.
 38. H. Nosrati, M. Salehiabar, E. Attari, S. Davaran, H. Danafar, H.K. Manjili, Green and one-pot surface coating of iron oxide magnetic nanoparticles with natural amino acids and biocompatibility investigation, *Appl. Organomet*. 2018 Sep; 32(2): 886-894. doi:10.1002/aoc.4069.

This work is licensed under a Creative Commons Attribution-NonCommercial 3.0 Unported License which allows users to read, copy, distribute and make derivative works for non-commercial purposes from the material, as long as the author of the original work is cited properly.